

# Generalized synchronization of chaos in non-invertible maps

V. Afraimovich<sup>a</sup>, A. Cordonet<sup>a</sup> and N.F. Rulkov<sup>b</sup>

<sup>a</sup> *IICO-UASLP, A. Obregón 64, 78000 San Luis Potosí, SLP, México*

<sup>b</sup> *Institute for Nonlinear Science, University of California, San Diego, La Jolla, CA 92093-0402*

(November 7, 2018)

The properties of functional relation between a non-invertible chaotic drive and a response map in the regime of generalized synchronization of chaos are studied. It is shown that despite a very fuzzy image of the relation between the current states of the maps, the functional relation becomes apparent when a sufficient interval of driving trajectory is taken into account. This paper develops a theoretical framework of such functional relation and illustrates the main theoretical conclusions using numerical simulations.

PACS number(s): 05.45.+b

## I. INTRODUCTION

Since the first studies by Van der Pol the dynamical theory of forced synchronization relates the synchronization phenomena to the onset of stable response behavior of driven oscillator [1–3]. As a result of this stability, the beats in the response oscillations disappear and a stable periodic motion occurs in the phase space of the driven oscillator. After that the oscillator becomes enslaved by the periodic forcing. Two main bifurcation scenarios that lead to the formation of the stable response behavior are the birth of stable limit cycle on a torus [2,4–7] and Andronov-Hopf bifurcation [2,8,9]. Based on these theoretical frameworks recent studies of synchronization in the chaotic oscillators have lead to the development of various notions of chaos synchronization. These notions include: identical synchronization [10–12], generalized synchronization [13–16], and phase synchronization [7,17,18].

An extension of the stability approach towards the case of directionally coupled non-identical chaotic oscillators is captured by the notion of generalized synchronization. The term, generalized synchronization, was introduced in [14] and used to describe the onset of synchronization in directionally coupled chaotic systems as the formation of a continuous mapping that transforms a trajectory on the attractor of the drive system into a trajectory of the response system. For the systems with invertible dynamics this is equivalent to the formation of a continuous mapping which links the current states of the systems when they are settled down on the synchronous attractor.

In the case of invertible dynamics of the driving system the relation between attracting properties of the response behavior and the some of the properties of the synchronization mapping has been reviled and proved [19–24]. In the case of non-invertible dynamics the relation between

the response stability and existence of the synchronization mapping was indirectly observed with the auxiliary method [25,26]. However, the detailed and rigorous study of this relation has not been done.

This paper presents the results of theoretical and numerical study of the onset of functional relation between the chaotic trajectories of driving non-invertible system and the states of the response system. Some results about this type of synchronization can also be found in [27,28]. To be specific we consider the systems in the form of the following maps

$$x_{n+1} = f(x_n), \quad (1)$$

$$y_{n+1} = g_c(x_n, y_n), \quad (2)$$

where equation (1) describes non-invertible driving system and equation (2) the response system. We assume for the sake of definiteness, that in the system (1), (2)  $x \in X \subset \mathbb{R}^m$  and  $y \in Y \subset \mathbb{R}^\ell$ , and that  $f$  and  $g_c$  are continuous. The subscript  $c$  stands for a coupling parameter. The global dynamics generated by the system (1), (2) can be written in the form  $F_c(x_n, y_n) = (x_{n+1}, y_{n+1})$ .

## II. THEORETICAL RESULTS

The non-invertibility of  $f$  implies that for any  $x_0 \in X$ , there are possibly infinitely many different backward orbits of  $x_0$  ( $x_0, x_{-1}, \dots, x_{-n}, \dots$ ). Let us denote by  $P(x_0)$  the union of all these possible backward orbits. Denote by  $p$  one of these orbits.

Assume that there exists a partition  $\{X_1, \dots, X_l\}$  of  $X$ , such that  $f|_{X_j}$  is one-to-one to the image\*. We define the backward symbolic sequence  $\alpha := (\alpha_0, \alpha_1, \dots, \alpha_n, \dots)$

---

\*The expression  $f|_{X_j}$  stands for the restriction of function  $f$

associated to a backward sequence  $(x_0, x_{-1}, \dots, x_{-n}, \dots)$  with  $\alpha_i = j$  if  $x_{-i} \in X_j$ .

Since we study synchronization in dissipative systems we also assume that there exists a ball of dissipation  $B \subset \mathfrak{R}^{m+\ell}$ , i.e.  $F_c(B) \subset \text{Int}(B)$  for any  $c \in S$ , where  $S$  is a region in the coupling parameter space in which system (2) has stable response behavior. Without loss of generality we assume that  $B = B_x \times B_y$ , i.e.  $B$  is a rectangle, where  $B_x$  (resp.  $B_y$ ) is a ball in the  $x$ -space (resp.  $y$ -space). Denote by  $\mathcal{A}_c$  the maximal attractor in  $B$ , i.e.  $\mathcal{A}_c = \bigcap_{n=0}^{\infty} F_c^n(B)$ . Assuming that system (2) has stable response behavior, we have

$$\lim_{n \rightarrow \infty} |y_n - \tilde{y}_n| = 0, \quad (3)$$

where  $(x_n, y_n) = F_c^n(x_0, y_0)$  ( $(x_n, \tilde{y}_n) = F_c^n(x_0, \tilde{y}_0)$ ) and  $(x_0, y_0), (x_0, \tilde{y}_0)$  are arbitrary points in  $B$ .

Let  $\mathcal{A}_{c,x} := \Pi_x \mathcal{A}_c$  be the image of  $\mathcal{A}_c$  under the natural projection  $\Pi_x$  to  $X$ . The set  $\mathcal{A}_{c,y}$  is the image of  $\mathcal{A}_c$  by  $\Pi_y$ , the natural projection to  $Y$ .

**Theorem 1.** *Under assumption of stable response given by Eq.(3) the attractor  $\mathcal{A}_c$  is the union of graphs of infinitely many functions. Each function  $h^\alpha$  is determined by a symbolic backward orbit  $\alpha$ . Moreover each  $h^\alpha$  is continuous.*

**Scheme of the proof.** The main point of the proof is to note that  $x_0$  and  $\alpha$  determine all the backward orbit  $p := (x_0, x_{-1}, \dots, x_{-n}, \dots)$ . From here the proof is similar to the one for the invertible case [23]. Given  $p$ , one can define  $h^\alpha(x_0)$  as the following limit:

$$h^\alpha(x_0) := \lim_{n \rightarrow \infty} \Pi_y F_c^n(x_{-n}, y)$$

independently of  $y \in B_y$ . This limit exists because of assumption (3).

Continuity is proved in the same way that in the invertible case taking into account that  $\alpha$  is the same for  $x$  and  $\tilde{x}$ , two close points in  $X$  (see [23] for details).  $\square$

Assume that the driving system is generated by a map  $f$  of the interval  $I$ . Then we can say more about regularity of branches provided that  $|y_n - \tilde{y}_n|$  goes to zero exponentially fast. Indeed the following proposition holds.

**Proposition 1.** *Assume that*

$$|y_n - \tilde{y}_n| \leq A\lambda^n, \quad (4)$$

where  $A > 0$  and  $0 < \lambda < 1$  are constants depending on  $c$ . Assume also that the one-dimensional driving system  $f$  is “hyperbolic”, i.e. there exists  $n_0$  such that  $(f^n)'(x) \geq \frac{1}{\gamma^-} > 1$  for all  $n \geq n_0$  and for any  $x$

for which the derivative exists. Then each branch  $h^\alpha$  is Lipschitz continuous.

**Scheme of the proof.**

The proof is basically the same of the one of theorem 7 in [23]. The point is to replace the space of Lipschitz functions  $H_{L,M}$  by  $H_{L,M,\alpha}$  with the restriction that the domain for  $h^\alpha \in H_{L,M,\alpha}$  consist of values of  $x$  compatible with  $\alpha$ .

Remark that by assumption, one has  $\gamma_- < 1$ . The condition (16) in theorem 7 in [23] can be replaced by

$$0 < A\lambda^n < \frac{1}{\gamma_-} \quad (5)$$

which is always true if  $n$  is large enough.  $\square$

Taking into account details of the proof of this proposition (which are omitted here and can be found elsewhere [23]) one might expect that if  $f$  is not hyperbolic then continuous synchronization functions  $h^\alpha$  could be not the Lipschitz-continuous functions. In this case the picture of individual branches  $h^\alpha$  might contain wrinkles and cups, and as the result, might appear fuzzy in numerical simulation due to finite resolution.

From now on we denote by  $h$  the union of all graphs  $h^\alpha$ . Each branch  $h^\alpha$  is only defined for the values of  $x$  compatible with  $\alpha$ . That is, if there is no backward orbit for the value  $x$  with the symbolic itinerary  $\alpha$ , then  $h^\alpha$  is not defined at  $x$ . Thus, in general, the number of branches of  $h$  is not necessarily the same for all  $x$ .

**Corollary to Theorem 1** *If  $\{X_i\}$  is a Markov partition then for any admissible  $\alpha$ , the domain of  $h^\alpha$  contains an element of  $\{X_i\}$ , i.e. if  $\alpha = (\alpha_0, \dots, \alpha_n, \dots)$  then  $D(h^\alpha) \supseteq X_{\alpha_0}$ .*

One may ask when two different branches of  $h$  are close. The next theorem shows that two branches that have similar recent history, are close to each other. Branches with different recent symbols could be either close or far from each other. As numerical simulations discussed in Sec.III we show that branches with different recent symbols may even intersect each other.

**Theorem 2.** *Let  $\{\tilde{\alpha}^i\}$  be a series of infinitely long symbolic sequences  $\tilde{\alpha}^i \in \{1, \dots, l\}^{\mathbb{N}}$  such that  $\lim_{i \rightarrow \infty} \tilde{\alpha}^i = \alpha$  in the standard product topology<sup>†</sup> [29]. Then,*

$$\lim_{i \rightarrow \infty} |h^{\tilde{\alpha}^i} - h^\alpha| = 0,$$

where  $|h^\beta| := \sup_{x \in D(\beta)} |h^\beta(x)|$

**Proof.**

---

to the partition element  $X_j$ . This type of partition is standard in the Markov maps of the interval, see for example [29].

---

<sup>†</sup>This means in particular that the greater is  $i$  the greater  $N$  first symbols in  $\alpha$  and  $\tilde{\alpha}^i$  coincide.

From (3), there exists an  $N$  such that for  $n \geq N$  and for any  $y_0$  and  $\tilde{y}_0$

$$|y_n - \tilde{y}_n| \leq \epsilon \quad (6)$$

This is, of course, true also for  $y_0, \tilde{y}_0 \in \mathcal{A}_{c,y}$ .

Now, choose  $i$  big enough in such a way that the first  $N$  symbols of  $\alpha$  and  $\tilde{\alpha}^i$  coincide. This means that  $(x, h^\alpha(x))$  and  $(x, h^{\tilde{\alpha}^i}(x))$  have the same first  $N$   $x$ -preimages  $(x_{-1}, \dots, x_{-N})$ . Then one can apply (6) for these points obtaining

$$|h^{\tilde{\alpha}^i}(x) - h^\alpha(x)| \leq \epsilon.$$

This is true for any  $x$  compatible with  $\alpha$  and  $\tilde{\alpha}^i$ . The theorem is proven.  $\square$

If one assumes monotonicity in assumption (3), that is,  $|y^n - \tilde{y}^n| \leq |Y|c^n$ , then a stronger result holds: Let  $\alpha$  and  $\tilde{\alpha}$  have the same first  $n$  symbols, then  $|h^\alpha - h^{\tilde{\alpha}}| \leq |Y|c^n$ .

Let us remark that there are three logical possibilities for the structure of the set  $h(x)$ : it could be finite, it could be countable, and it could contain a Cantor set.

The first possibility trivially occurs in the case of identical synchronization, that can exist even for non-invertible  $f$  (see for instance [23]).

The second possibility can be justified by construction of a special pair  $f, g_c$ . We believe that it could be done. It is definitely true for the case when  $f$  has zero topological entropy, i.e. the number of admissible words  $\{\alpha_0, \dots, \alpha_{n-1}\}$  grows subexponentially as  $n$  goes to infinity. For example, if the topological Markov chain corresponding to a Markov partition  $\{X_j\}$  has zero topological entropy then the number of admissible words grows not faster than polynomially. If topological entropy is positive then the construction of such an example is rather difficult, we are going to study this problem elsewhere.

The third possibility seems to be generic in a space of pairs of functions  $f, g_c$  provided that  $f$  has positive topological entropy. It seems natural to believe that different driving signals correspond to different outputs in the regime of synchronization. Numerical simulations considered in Sec.III confirm this conjecture (see also Fig. 3 in [27] and Fig. 2d in [28]). However, we do not have a rigorous proof of this statement right now.

The statements made above give a clear picture of the underlying structure of generalized synchronization of chaos in the case when the dynamics of drive system is non-invertible.

### III. SYNCHRONIZATION FUNCTION IN NON-INVERTIBLE MAPS: EXAMPLE

To illustrate the properties of generalized synchronization in non-invertible maps consider the synchronization

of logistic map driven by tent map. In this case function  $f(x_n)$  in the driving system (1) is of the form

$$f(x) = \begin{cases} x/b & \text{if } x < b, \\ (x-1)/(b-1) & \text{if } x \geq b, \end{cases}$$

where  $b$  is a control parameter,  $0 < b < 1$ . We will consider the case when the dynamics of the response system is given by the following map

$$y_{n+1} = (1 - \epsilon)ay_n(1 - y_n) + \epsilon f(x_n), \quad (7)$$

where  $a$  is the control parameter of the map and  $\epsilon \in [0, 1]$  is a coupling parameter. Note that upper bound of the contraction rate in the  $y$ -direction denoted by  $c$  in previous section is, in this case,  $c = (1 - \epsilon)a$ . In the numerical simulation considered in this section the values of control parameters are fixed  $b = 0.677$  and  $a = 3.7$ .

Since the dynamics of the maps are different, the generalized synchronization is the only possible regime of synchronization, except to the trivial case when  $\epsilon = 1$ . The onset of generalized synchronization is detected with auxiliary system approach. In this analysis we study the stability of the chaotic response attractor in the manifold  $y_n = z_n$ , where variable  $z_n$  is described by an exact replica of the system (7) which is called auxiliary system [25].

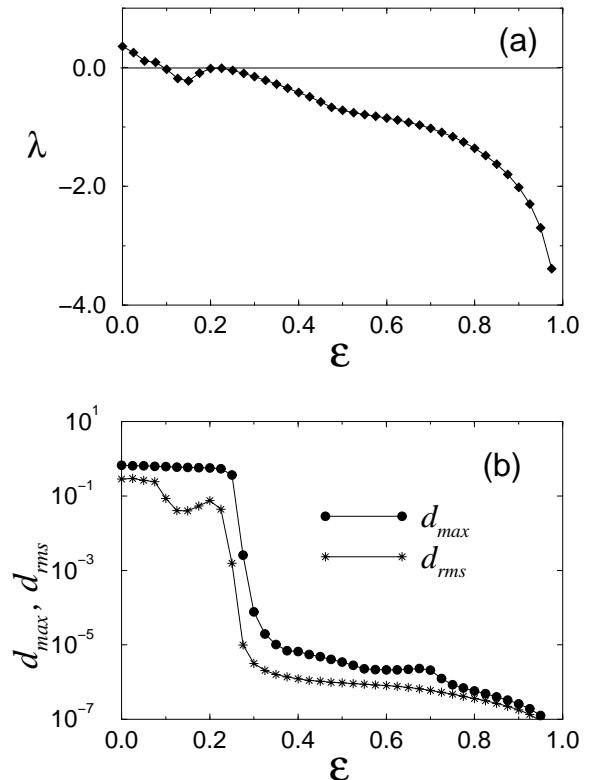


FIG. 1. The dependance of conditional Lyapunov exponent  $\lambda$  on the value of coupling parameter  $\epsilon$  - (a), and the values of maximal and rms deviations of  $d_n$  computed as a function of  $\epsilon$  - (b).

It can be shown with the analysis based on contraction mapping [30] that stable identical oscillations in response and auxiliary systems are guaranteed when the values of coupling parameter are within the interval  $1 - 1/a_l < \epsilon < 1 + 1/a_r$ , where  $a_l = a(1 - 2y_n^{min})$ ,  $a_r = a(1 - 2y_n^{max})$ , and  $y_n^{min}$  and  $y_n^{max}$  are the leftmost and rightmost points of the attractor in the response system. This indicates that if for the selected parameter values of the maps the coupling is stronger than  $\epsilon = 0.7$ , then synchronization is monotonically stable.

More precise evaluation of the synchronization threshold can be done with the analysis of conditional Lyapunov exponents (see, Fig 1a) and with the analysis of deviation of response-auxiliary system from manifold  $y_n = z_n$ . The dependance of maximal,  $d_{max}$ , and rms,  $d_{rms}$ , values of deviation  $d_n = z_n - y_n$  on the values of coupling parameter are presented in Fig. 1b.

Based upon the plots in Fig. 1 one would expect that the regime of generalized synchronization takes place for the coupling parameter values  $\epsilon > 0.3$ . This regime assumes existence of a continuous functional relation between the trajectories  $x_n$  and  $y_n$ . However, when one plots the states of the one-dimensional phase space  $y_n$  on the synchronized attractor versus the corresponding states of one-dimensional phase space  $x_n$ , the image of such relation looks fuzzy, see Fig. 2. It is clear that point to point mapping  $x_n \rightarrow y_n$  cannot be interpreted as a continuous function.

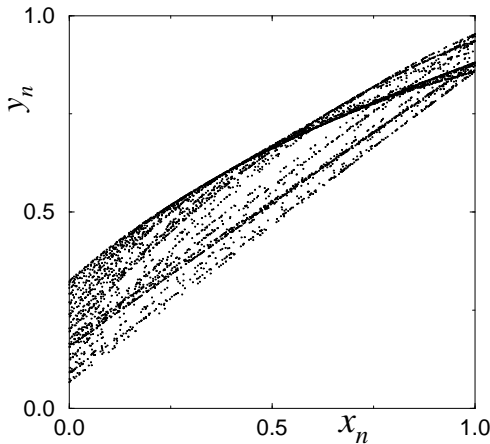


FIG. 2. Synchronized chaotic attractor computed for  $\epsilon = 0.6$  plotted in the phase plane  $(x_n, y_n)$ .

In order to unveil the synchronization function in the numerical analysis we consider the mapping  $(x_n, [\alpha_1, \dots, \alpha_m]) \rightarrow y_n$ , where  $\alpha_k$  are symbolic representation of prehistory of the trajectory  $x_n$ . These symbols are generated by the tent map (1) which is partitioned into two regions:  $\alpha_k = L$  if  $x_{n-k} < b$  and  $\alpha_k = R$  if  $x_{n-k} \geq b$ . The points of the synchronous attractor whose preceding symbolic sequence of the driving trajectory has a specific sequence (a mask) were selected

and analyzed separately. This analysis shows that as the length of the sequence increases the cloud of points shrinks into a curve. An example of such convergence is illustrated in Fig. 3, where the mask of 8 symbols  $[L, L, R, L, L, R, R, R]$  is studied. Similar behavior is observed for the other sequences of the same length. In the sequences of this length the shape of the curve varies as the symbolic sequence changes. All together these curves form the fuzzy shape of the synchronized attractor shown in Fig.2.

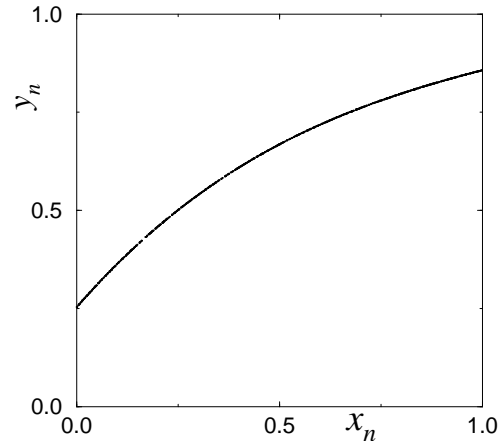


FIG. 3. Points of the synchronized chaotic attractor shown in Fig. 2 generated by the trajectories which symbolic sequence of length  $m = 8$ , preceding the final point  $x_n$ , fits to the mask  $[L, L, R, L, L, R, R, R]$ .  $\epsilon = 0.6$

To evaluate the convergence of the image of synchronized attractor to a continuous function  $h^\alpha(x)$  we analyzed the sets of attractor points conditioned by all possible symbolic masks  $\alpha$  of various length  $m$ . For each mask of preceding symbols  $S_m^i = [\alpha_1, \dots, \alpha_m]$  we computed the best polynomial fitting function  $\phi_{S_m^i}(x)$  of order 6 using Singular Value Decomposition (SVD) algorithm, and studied the dependance of mean squared error (MSE), averaged over all masks of length  $m$ , versus  $m$ . This dependence computed for the values of coupling parameter  $\epsilon = 0.6$  and  $\epsilon = 0.4$  are shown in Fig. 4.

One can see from the Fig. 4 that MSE decreases exponentially fast when  $m$  increases. Approximating this dependence with exponent

$$MSE(m) \sim e^{\Lambda m}, \quad (8)$$

one can find the rate of convergence, which is in the case  $\epsilon = 0.6$  equals  $\Lambda \approx -1.05$ .

Figure 5 shows how the convergence rate  $\Lambda$  depends on the value of coupling parameter  $\epsilon$ . Comparing this plot with the plot of conditional Lyapunov exponent versus  $\epsilon$  one can clearly see the similarity in these plots. This is indicative of the fact that in the generalized synchronization regime in our case the convergence rate  $\Lambda$  is

related to the contraction rate of response system given by conditional Lyapunov exponent  $\lambda$ . This relation was defined for the case of monotonic stability of the response behavior, see Section II.

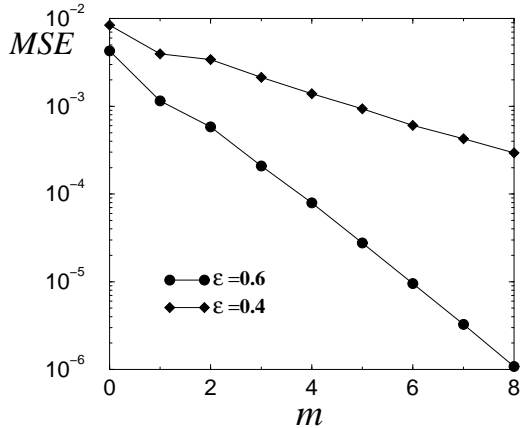


FIG. 4. The dependence of MSE of best polynomial fitting function for the attractor points  $y_n, x_n$  on the length  $m$  of the preceding masks  $S_m^i$ .

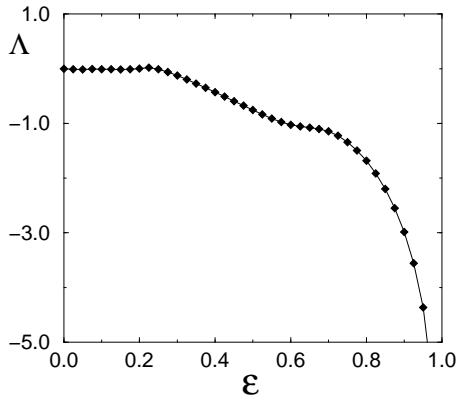


FIG. 5. The dependence of the convergence rate  $\Lambda$  on the value of coupling parameter  $\epsilon$ .

One can see from Fig.2 that synchronization mapping for the current states of the drive and response system has a complex structure of branches. The appearance of Cantor set in the synchronized attractor caused by non-invertible driving system was reported before in [28]. The formation of the fractal structure can be explained by the analysis of deviations of the branch caused by the change of symbol  $\alpha_n$  appeared in the symbolic sequence  $n$  iterations before. For the most of the driving trajectories, the stability of the response behavior acts in a such way that the deviation will be reduced with the increasing value of  $n$ . As the result the deviations of different scales for different values of  $n$  are responsible the formation of the complete structure of the synchronized attractor. This

explains the formation of fractal structure in the synchronization mapping which consists of infinite number of the branches.

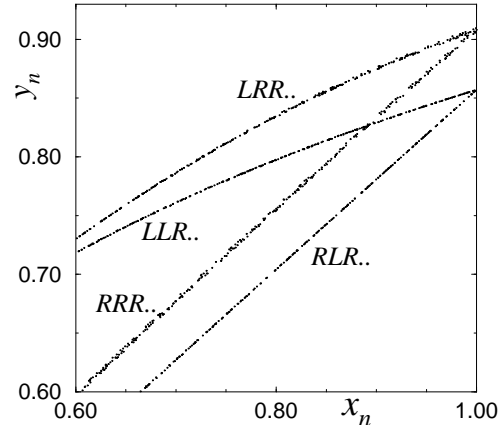


FIG. 6. Branches of the synchronized chaotic attractor shown in Fig. 2 computed for symbolic sequences of length  $m = 8$ ,  $[\alpha_1, \alpha_2, R, L, L, R, R, R]$ . The values of three most recent symbols  $\alpha_1, \alpha_2, R$  are shown next to the corresponding branch.

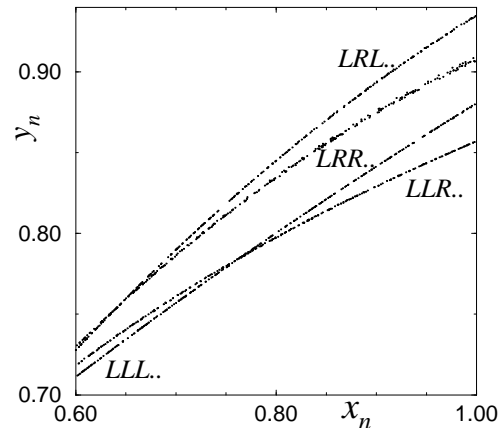


FIG. 7. Branches of the synchronized attractor for the sequences  $[L, \alpha_2, \alpha_3, L, L, R, R, R]$ . The values of three most recent symbols  $L, \alpha_2, \alpha_3$  are shown next to the corresponding branch.

This mechanics behind the formation of Cantor set is illustrated in Figs. 6 and 7. Figure 6 shows the set of points of the synchronized attractor corresponding to the trajectories whose 8 most recent symbols are fixed. One can see that branches with the same most recent symbols remain relatively close to each other, while the branches with different most recent symbols can get apart significantly. The similar situation takes place for the alternation of the more remote symbols, see Fig. 7. However the scale of the deviation in this case is less than in Fig. 6. Further increase of the length of alternating symbols by one in considered mask of symbols the number

of branches doubles. The new branches appear close to the branches with the same most recent symbols. Continuation of this process with infinitely long mask  $n \rightarrow \infty$  leads to the formation of a fractal, Cantor type set.

#### IV. CONCLUSIONS

The results of the theoretical analysis of synchronization presented in Sec. II and the numerical analysis of particular example considered in Sec. III allow one to draw a number of important conclusions on typical properties of synchronization mapping that characterize generalized synchronization of chaos in the case of non-invertible driving system.

The synchronization mapping, in this case, can be interpreted as a continuous function only when all backward iterations  $x_{-n}$  of the driving trajectory  $x_0$  are included in the vector of the function arguments. We have shown that Markov partition of the driving map can be used to describe the backward iterations in a compact symbolic way. The set of points of synchronization mapping plotted for the trajectories, which prehistory is conditioned by a selected sequence of symbols, asymptotically approach the graph of a continuous function as the length of the sequence increases.

The set of these graphs given by all possible symbolic sequences of infinite length form the complex fuzzy object which is typically observed in the joint phase space of the one-dimensional chaotic maps synchronized in the generalized sense.

An interesting feature of the considered example with 1-d maps is that branches  $h^\alpha$  remain smooth functions even when the rate of conditional stability is rather weak. Indeed, according to the papers [19–24], one would expect that  $h^\alpha$  would become non-differentiable, Hölder continuous function as the contraction rate in the response system becomes lower than some critical value. However, this critical value is given by a contraction rate towards the chaotic attractor in the driving system. In our case the driving trajectories of the 1-d map with the specified symbolic sequence  $\alpha$  do not have contracting direction. They have only unstable direction. As the result the contraction rate in the response system for any given branch  $h$  is always stronger than in the driving system.

This feature is typical for the driving systems in the form of one-dimensional hyperbolic map. In the case of non-hyperbolic 1-d driving map function  $h^\alpha$  may become non-differentiable and contain wrinkles and cusps. Another interesting question arises when one considers a system without exponential stability or Markov partition? It could be expected that branches become non-differentiable. For the moment the question is open.

#### V. ACKNOWLEDGMENT

This work was supported in part by a grant from the University of California Institute for Mexico and the United States (UC MEXUS) and the Consejo Nacional de Ciencia y Tecnología de México (CONACYT). A.C. would like to thank the members of the INLS for their hospitality during his visit to San Diego. A.C. is supported by a CONACYT-ECOS-Nord contract. N.R. was supported in part by U.S. Department of Energy (grant DE-FG03-95ER14516), the U.S. Army Research Office (MURI grant DAAG55-98-1-0269).

- 
- [1] B. van der Pol, *Philos. Mag.*, **3**, 65 (1927).
  - [2] A.A. Andronov and A.A. Witt, *Atch. Electrotech* **16** (4), 280 (1930).
  - [3] N. Minorsky, *Nonlinear oscillations*, [Huntington, N.Y., R. E. Krieger Pub. Co.], 1974 [c1962], 714.
  - [4] V.I. Arnold, *Mathematical Methods of Classical Mechanics*, [Springer-Verlag, Berlin], 1974.
  - [5] V.S. Afraimovich and L.P. Shil'nikov. in *Methods of the Qualitative Theory of Differential Equations*, [Gorky University Press, Gorky], 1983, pp.3-26.
  - [6] J.A. Glazier and A. Libchaber. *IEEE Trans. Circ. and Sys.*, **35**, 790 (1988)
  - [7] A. Pikovsky, M. Rosenblum, and J. Kurths. *Int. J. Bifurcation and Chaos*, **10**, 2291 (2000)
  - [8] P. Holmes and D.R. Rand. *Quart. Appl. Math.* **35**, 495 (1978)
  - [9] R. Mettin, U. Parlitz, and W. Lauterborn. *Int. J. Bifurcation and Chaos*, **3**, 1529 (1993)
  - [10] H. Fujisaka and T. Yamada. *Prog. Theor. Phys.* **69**, 32 (1984)
  - [11] L.M. Pecora and T.L. Carroll. *Phys. Rev. Lett.* **64** (1990), 821-824.
  - [12] N.F. Rulkov, *CHAOS*, **6**, 262 (1996).
  - [13] V. Afraimovich, N.N. Verichev and M.I. Rabinovich, *Radiophys. Quant. Electr.* **29**, 747 (1986).
  - [14] N.F. Rulkov, M.M. Sushchik, L.S. Tsimring, and H.D.I. Abarbanel, *Phys. Rev E* **51**, 980 (1995).
  - [15] L.M. Pecora, T.L. Carroll, and J.F. Heagy, *Phys. Rev E* **52**, 3420 (1995).
  - [16] L. Kocarev and U. Parlitz, *Phys. Rev. Lett.* **76**, 1816 (1996).
  - [17] A. Pikovsky *et al.*, *Chaos* **7**, 680 (1997)
  - [18] M.A. Zaks *et al.*, *Phys. Rev. Lett* **82**, 4228 (1999).
  - [19] B.R. Hunt, E. Ott and J.A. Yorke, *Phys Rev. E* **55**, 4029 (1997).
  - [20] J. Stark, *Invariant graphs for forced systems*, *Physica D* **10** (1997), 163-173.
  - [21] J. Stark, *Regularity of invariant graphs for forced systems*, *Ergod. Th. & Dyn. Syst.* **19** (1999) 155-199.
  - [22] K. Josić, *Phys. Rev. Lett.* **80**, 3053 (1998).
  - [23] V. Afraimovich, J.-R. Chazottes, and A. Cordonet, *Dis-*

- crete and Continuous Dynamical Systems: Series B **1**, 421 (2001).
- [24] K. Josić, *Nonlinearity*. **13**, 1321 (2000).
  - [25] H.D.I. Abarbanel, N.F. Rulkov and M.M. Sushchik, *Phys. Rev. E* **53**, 4528 (1996).
  - [26] K. Pyragas, *Phys. Rev. E* **54**, R4508 (1996).
  - [27] J. Chubb *et al.*, *Int. J. Bifurcation and Chaos*, **11**, 2705-2713 (2001)
  - [28] P. So *et al.* *Phys. Rev. E* **65**, 046225 (2002)
  - [29] Kitchens, B., *Symbolic dynamics: one-sided, two-sided, and countable state Markov shifts.* (Springer, 1998).
  - [30] Yu. I. Neimark, *The Method of Point Mappings in the Theory of Nonlinear Oscillations.* (Moscow: Nauka, 1972) [in Russian].